HOKKAIDO UNIVERSITY

Title	DYNAMIC RESPONSE CHARACTERISTICS OF THE TALL NOISE BARRIER ON RAILWAY STRUCTURES DURING SEISMICITY
Author(s)	TOKUNAGA, M.; SOGABE, M.; WATANABE, T. et al.
Description	The Thirteenth East Asia-Pacific Conference on Structural Engineering and Construction (EASEC-13), September 11-13, 2013, Sapporo, Japan.
Relation	Proceedings of the Thirteenth East Asia-Pacific Conference on Structural Engineering and Construction (EASEC-13), September 11-13, 2013, Sapporo, Japan, F-1-6.
Citation	Proceedings of the Thirteenth East Asia-Pacific Conference on Structural Engineering and Construction (EASEC-13), F-1-6
Issue Date	2013-09-12
Doc URL	https://hdl.handle.net/2115/54372
Type	conference paper
File Information	easec13-F-1-6.pdf

Hokkaido University Collection of Scholarly and Academic Papers

Hokkaido University Collection of Scholarly and Academic Papers : HUSCAP

DYNAMIC RESPONSE CHARACTERISTICS OF THE TALL NOISE BARRIER ON RAILWAY STRUCTURES DURING SEISMICITY

M. TOKUNAGA[1*], M. SOGABE[1†], T. WATANABE, T. SANTO[2] and S. TAMAI[2]

[1]*Structural Mechanics Laboratory, Railway Technical Research Institute, Japan*
[2]*Design and Technology Department, Japan Railway Construction, Transport and Technology Agency, Japan*

ABSTRACT

The tall noise barriers recently installed on Shinkansen structures have a low natural frequency. Therefore, they may resonate with dynamic loads such as seismicity which have not been a crucial condition for their design. The aim of this study is to understand the dynamic response characteristics of the tall noise barrier during seismicity and to evaluate its seismic safety. Conclusions on the basis of numerical studies are as follows: 1) the noise barrier resonates with the yield frequency of structures during the L2 earthquake, while it resonates with the elastic natural frequency of structures when structures respond elastically in such cases as L1 earthquake. This phenomenon becomes significant with the increase of the seismic yield coefficient. 2) In order to evaluate the seismic response of noise barrier, it is necessary to take account of the influence of the dynamic interaction between the noise barrier and the structure, because the transfer function of the noise barrier substantially depends on the interaction. 3) The L1 earthquake can cause cracks at the top of bridge railing, and the L2 earthquake can cause the yield of H-section steel which supports the noise barrier. 4) The L2earthquake can provide a severer design condition than the wind load for the noise barrier whose natural frequency is 5Hz or less.

Keywords: Noise barrier, Seismic Safety, Railway Viaducts, Resonance

1. INTRODUCTION

Noise barriers are provided on high-speed railway structures for the noise reduction depending on the land use along railway lines. Those which consist of H-shaped steel struts and precast PC plates have come to be used frequently with a view of construction cost reduction and labor-saving construction. In the design of H-shaped steel struts which determine the structural performance of the noise barrier, various effects have to be taken into account such as the train wind, the fatigue, the propulsive force on the bridge railing, the flying snow caused by running train and the wind load which often becomes a crucial condition for design (RTRI 2004).

On the other hand, the effect of the earthquake which is the main topic in this paper has not been a crucial condition in practice design because it is considered as static actions of only k_h=0.7, assuming the yield seismic coefficient of railway viaducts.

In recent years, development need of tall noise barriers has been increased with the progress of new Shinkansen

* Presenter: Email: toku@rtri.or.jp

† Corresponding author: Email: toku@rtri.or.jp

lines construction. In terms of the practical application, the dynamic response amplification of such tall noise barrier due to resonance with structures and ground motions is a concern, because its natural frequency becomes lower than the conventional noise barrier. The dynamic response of OCS poles which are also structures incidental to the line has been investigated in the previous study (Imamura 2007; Murono 2012).

In addition, in the previous study by the authors, the fracture morphology of a noise barrier has been revealed on the basis of the detailed finite element model, and its dynamic response during earthquakes has been evaluated (Tokunaga 2011). However, the interaction between the noise barrier and the structure, or resonance phenomenon between them when structures respond elastically in case of L1 earthquake has not be mentioned in detail.

In order to understand the dynamic response characteristics of the tall noise barrier during seismicity and to evaluate its seismic safety, the following items have been investigated in this paper. 1) To evaluate the effect of elastic natural frequency of structures on the seismic response of the noise barrier. 2) To evaluate the effect of the interaction between noise barriers and structures on the seismic response of the noise barrier. 3) To assess the seismic response and fracture morphology of the target noise barrier, and to clarify the seismic safety.

2. ANALYSIS METHOD

2.1. Target noise barrier and structure

Figure 1 shows the cross-section of the semi-cover snow storing type noise barrier to be discussed in this paper. The height of the noise barrier *H* is Rail Level (hereinafter referred to as "R.L.")+3.5m. It consists of cavity prestressed concrete boards (hereinafter referred to as "PC board") and H-shaped steel which is arranged at 3m intervals on bridge railings.

Target structures are rigid viaducts with the standard design and wall type piers which often have the noise barriers. Since the seismic response of the noise barrier is greatly influenced by the vibration characteristics of structures, vibration characteristics of 52 rigid viaducts and 39 wall type piers which are typical in the line section were statistically surveyed on the basis of the design drawings.

Figure 2 shows the vibration characteristic survey results on the basis of pushover analysis from design

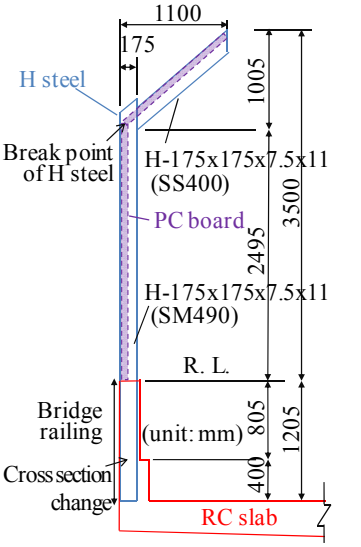

Figure 1: Cross-section of noise barrier

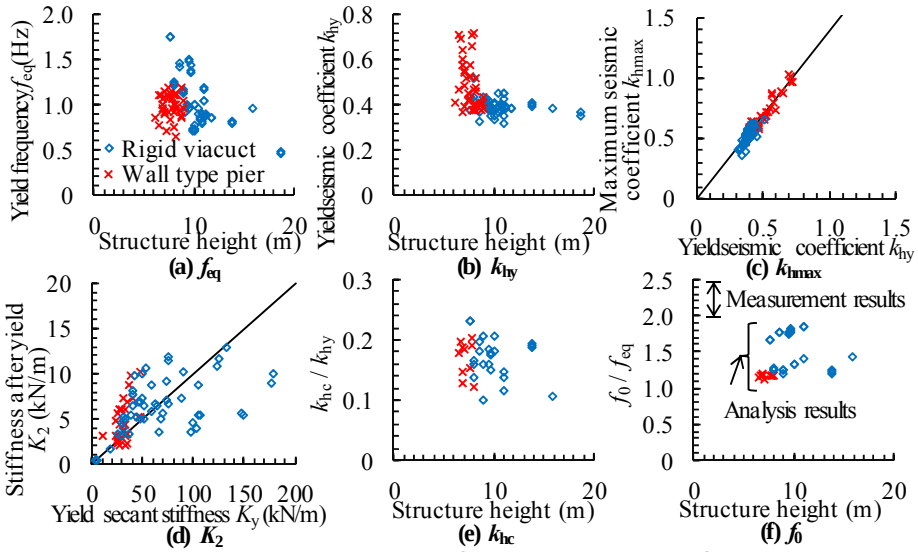

Figure2: Vibration characteristic on the basis of pushover analysis results from design documents

documents. As shown in Figure 2(a), the yield frequency f_{eq} which is the inverse of the equivalent natural period is distributed in a range of 0.5~2.0Hz for the rigid viaduct and in a range of 0.6~1.3Hz for the wall type pier. As shown in Figure 2(b), the yield seismic coefficient k_{hy} is distributed in a range of 0.3~0.5 in the rigid viaduct and in a range of 0.3~0.7 for the wall type pier. As shown in Figure 2(c), a ratio of k_{hmax}/k_{hy} is around 1.4 regardless of structure type. A ratio of the stiffness after yield K_2 to the yield point secant stiffness K_y is generally about 0.1 on an average. As shown in Figure 2(d), the seismic coefficient k_{hc} and the elastic natural frequency f_0 which correspond to the stiffness reduction point due to the cracking occurrence (hereinafter referred to as "C point ") were extracted from the skeleton curve. As shown in Figure 2(e), a ratio of k_{hc}/k_{hy} is from 0.1 to 0.2. In addition, a ratio of f_0/f_{eq} ranges from 1.0 to 2.0 approximately although, in the previous study based on the microtremor measurement by the authors, the value ranges from 2.0 to 2.5 approximately (Tokunaga 2011). This is because the soil stiffness value of actual structures measured during a small vibration is 4-10 times larger than the value used in seismic design. This study adopted the measurement results to set the initial stiffness of the structure.

2.2. Detailed model (for limit value)

Figure 3 shows the detailed analysis model for evaluating the limit value and the fracture morphology of the noise barrier. H-shaped steel and concrete were modeled by solid elements. Longitudinal reinforcements and additional reinforcements were modeled by beam elements. Tie hoops were modeled by embedded elements.

Figure 4 shows the relationship of stress-strain of concrete, steel and reinforcement. As for concrete elements, Young's modulus E was set at 2.65×10^4(N/mm^2) and Poisson's ratio ν was set at 0.3. The compression softening property of the concrete element was set on the basis of the curved section in the reference(RTRI 2004) up to the maximum stress (ε_0=2000μ strain), and was set to a linear softening line on the basis of the compression fracture energy after the maximum stress. The tensile softening property was modeled by Hordijk equation considering the tensile breaking energy. Compression fracture energy G_{Fc} was calculated from the equation by Nakamura et al. (Nakamura 2001). As for steel and reinforcement elements, Young's modulus E was set at 2.0×10^5(N/mm^2), and Poisson's ratio ν was set at 0.2, and Von

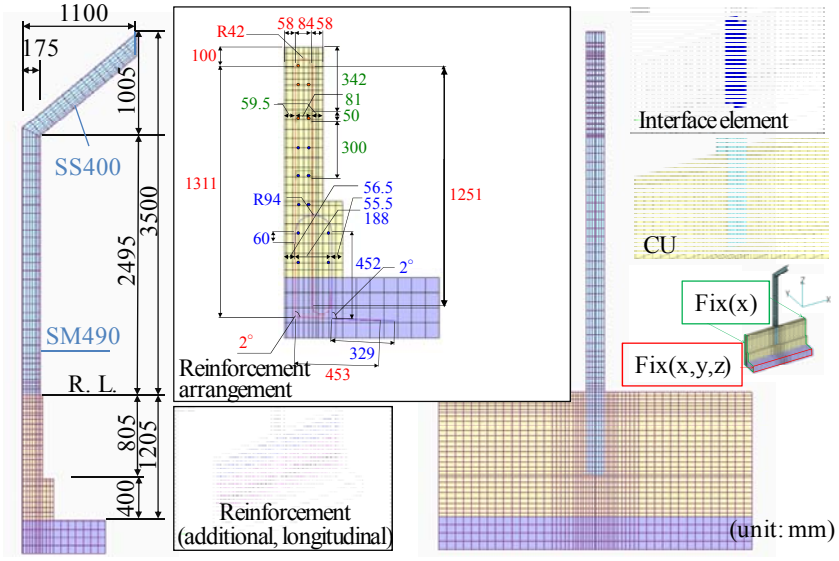

Figure 3: Analysis model of the detailed model (limit value)

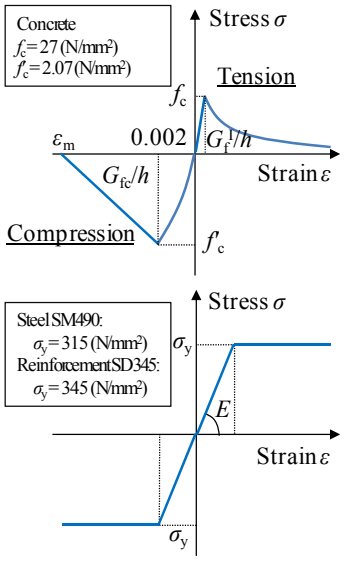

Figure 4: Relationship of stress-strain

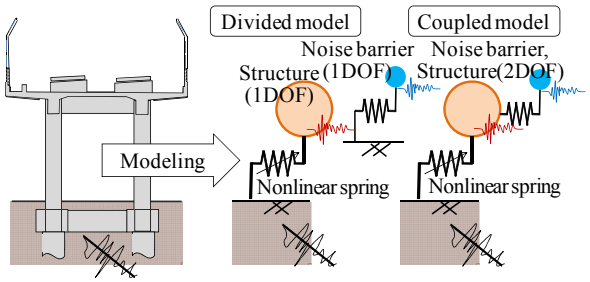

Figure 5: Analysis model of the detailed model (response value)

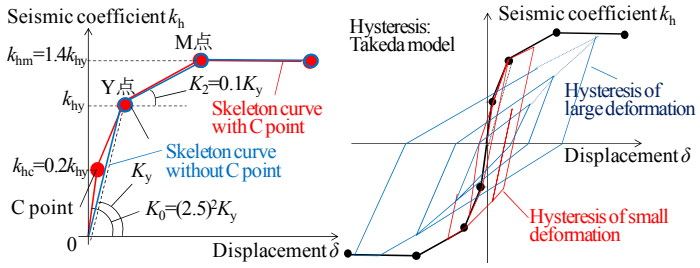

Figure 6: Non-linear spring characteristics

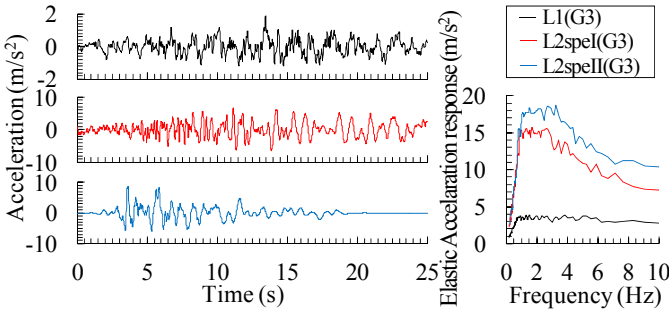

Figure 7: Time history waveforms and elastic response spectra of earthquakes

Table 1 : Analysis cases

Detailed model (limit value)	Load direction		Positive side (track side) Negative side (outside)
Overall model (response value)	Input earthquake		L1, L2speI, L2speII (G3ground)
	Structure	f_{eq} (Hz)	0.4, 0.6, …, 3.0
		k_{hy}	0.5, 0.6, …, 1.0
		C point	Considering, Non-considering
		Interaction	Divided, Coupled (Weight ratio α_{nbr}=1,10,100)
	Noise barrier	f_{nbr} (Hz)	1.0, 1.5, 2.0, …, 10

Mises yield condition and a wholly elastic-plastic model were used. Reinforcement and concrete were modeled by assuming the full adhesion. After reproducing the initial force due to the weight, static inertia force was gradually increased in the lateral direction.

2.3. Overall model (for response value)

2.3.1. Analysis model

Figure 5 shows the analysis model of the overall model for calculating a response value of the seismic noise barrier. Structures and noise barriers were represented with a single degree of freedom respectively. The response of the structures was modeled with a non-linear spring and a linear damper and that of the noise barriers was modeled with a linear spring and a linear damper. A coupled model to take into account the dynamic interaction between the noise barriers and the structures and a divided model without considering the interaction were prepared. The modal damping ratio of the structures and the noise barriers were set at 5% and 2% respectively.

Figure 6 shows non-linear spring characteristics of the structure that are set based on the results of statistical surveys of the section **2.1**. The skeleton curve with or without C point were adopted. C point was set based on k_{hc}=0.2k_{hy} and f_0=2.5 f_{eq} and M point was set based on k_{hmax}=1.4k_{hy} and K_2=0.1K_y. As for the hysteresis of structures, Takeda model (Takeda 1970) was adopted that can represent the precise response of the concrete members that railway structures commonly have.

2.3.2. Seismic wave

Figure 7 shows time history waveforms and elastic response spectra of the earthquakes used for the analysis with the overall model. 3 design earthquakes, L1, L2 spectrum I, L2 spectrum II used for dense soil (hereinafter referred to as "L1(G3)", "L2speI(G3)" and "L2speII(G3)" respectively) were adopted (RTRI 2012).

2.3.3. Analysis cases

Table 1 shows analysis cases. In the detailed model for the calculation of the limit value, there are two

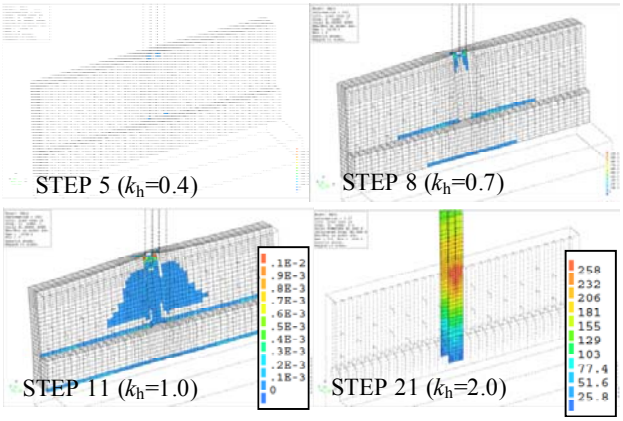

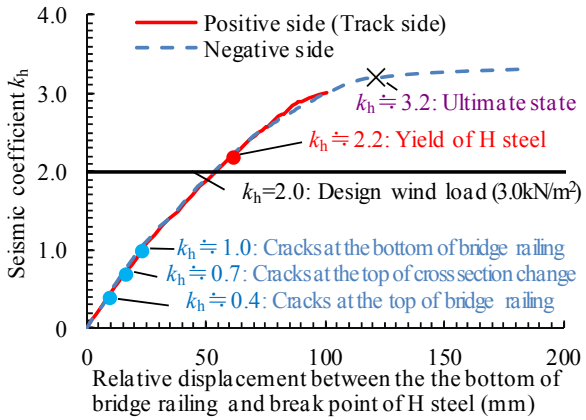

Figure 8: Von Mises stress distribution and cracking distribution **Figure 9: Relationship between seismic coefficient and displacement**

cases of loading direction, the positive side (track side) and the negative side (outside). The overall model for the response value was investigated based on the parameters of f_{eq}=0.4~3.0Hz, k_{hy}=0.5~1.0, the C point and the interaction. In order to evaluate the effect of the interaction, the divided mode and the coupled model whose weight ratio α_{nbr} of the noise barrier to the structure varies in 1,10 and 100 were used as shown in Figure 5. The natural frequency of the noise barrier f_{nbr} was 1~10Hz.

3. ANALYSIS RESULTS

3.1. Limits and fracture morphology of noise barrier

Figure 8 shows the Von Mises stress distribution of H-shaped steel (STEP 21) and cracking distribution in concrete elements (STEP 5, 8 and 11), which were obtained from the analysis results of the detailed model. As shown in the figure, cracks at the top of bridge railing can be observed when the seismic coefficient becomes about 0.4 in both the cases of the positive side loading and the negative side loading. Then, cracks spread to the discontinuous changing position of the cross section along the H-shaped steel when the seismic coefficient becomes about 0.7 and it reaches the bottom of bridge railing in the direction of 45° when the seismic coefficient becomes about 1.0. From the Von Mises stress distribution of H-shaped steel, H-shaped steel exceeds the yield stress 315N/mm^2 at the junction of a web and a compression flange near the top of bridge railing when the seismic coefficient becomes about 2.2. A plastic zone spreads to the entire compression flange near the top of bridge railing when the seismic coefficient becomes about 2.5. Thereafter, the deformation rapidly increases to the ultimate limit state because H-shaped steel cannot be hold the load bearing capacity. In this paper, the point seismic coefficient 3.2 where the deformation increases rapidly was supposed to be the ultimate state.

Figure 9 shows the relationship between seismic coefficient and displacement obtained from pushover analysis of the detailed model. The relative displacement between the bottom of bridge railing and break point of H-shaped steel is plotted along the horizontal axis. From the figure, it can be confirmed that the noise barrier behaves elastically until seismic coefficient reaches about 1.0, and comes to the ultimate state due to large deformation when the seismic coefficient reaches 2.5 or lager. The behavior is similar in both the cases of the positive side loading and the negative side loading. Considering that the design wind load (3.0kN/m^2) which becomes the most dominant design conditions in the current design of the noise barrier corresponds to the seismic coefficient 2.0, it

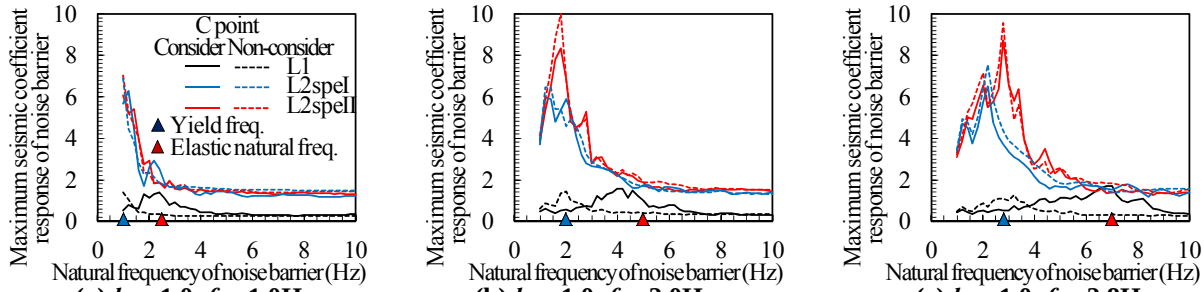

(a) k_{hy}=1.0, f_{eq}=1.0Hz (b) k_{hy}=1.0, f_{eq}=2.0Hz (c) k_{hy}=1.0, f_{eq}=2.8Hz

Figure 10: Effect of the presence or absence of C point on seismic response of noise barrier (α_{nbr}=100)

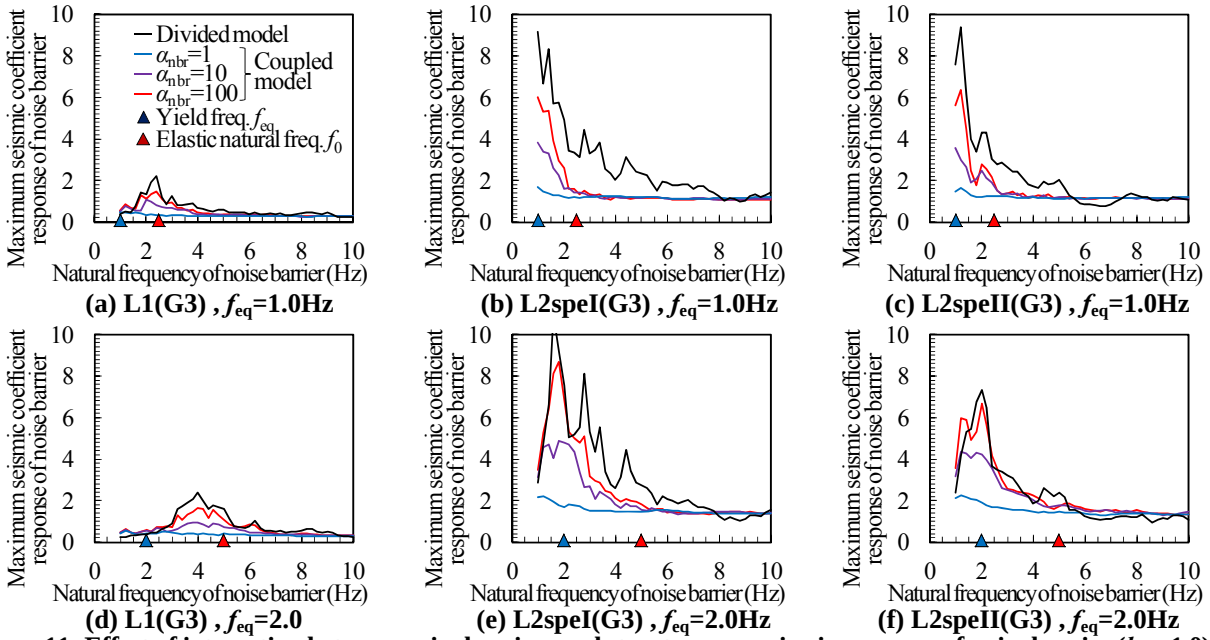

(a) L1(G3) , f_{eq}=1.0Hz (b) L2speI(G3) , f_{eq}=1.0Hz (c) L2speII(G3) , f_{eq}=1.0Hz

(d) L1(G3) , f_{eq}=2.0 (e) L2speI(G3) , f_{eq}=2.0Hz (f) L2speII(G3) , f_{eq}=2.0Hz

Figure 11: Effect of interaction between noise barriers and structures on seismic response of noise barrier (k_{hy}=1.0)

can be confirmed that H-shaped steel doesn't reach the yield state against wind load as expected in the design. Incidentally, the natural frequency corresponding to the point of seismic coefficient 0.5 was 3.3Hz.

3.2. Seismic response of noise barrier

Figure 10 shows the maximum seismic coefficient response of the noise barrier which indicates the effect of the presence or absence of the C point on the basis of the results of the coupled model with a weight ratio α_{nbr}=100. The value of seismic coefficient was calculated from the ratio of the linear spring force to the noise barrier weight. As shown in the figure, in the case without C point, the maximum response of the noise barrier marks large value when the natural frequency of noise barrier f_{nbr} and f_{eq} match to each other. On the other hand, in the case with C point, it is increased when f_{nbr} is in a range between from f_{eq} to f_0 during L1 earthquake although it is increased when f_{nbr} is equivalent to f_{eq} during L2 earthquake. Thus, it can be found out that the noise barrier resonates with the yield frequency of structures during the L2 earthquake, while it resonates with the elastic natural frequency of structures when structures respond elastically in such cases as L1 earthquake. This phenomenon becomes significant with the increase of the seismic yield coefficient. In addition, in the case where k_{hy}=1.0 and f_{eq}=2.8Hz such as the case of short wall type piers, it can be observed that the response of noise barrier, during L1 earthquake, becomes about 1.8 which is equal to or greater than that during L2 earthquake when f_{nbr} is generally consistent with the f_0. Therefore, if the structure responds elastically, it is necessary to take account of the stiffness decrease of the structure from the initial value due to cracks in order to evaluate the response of noise barriers.

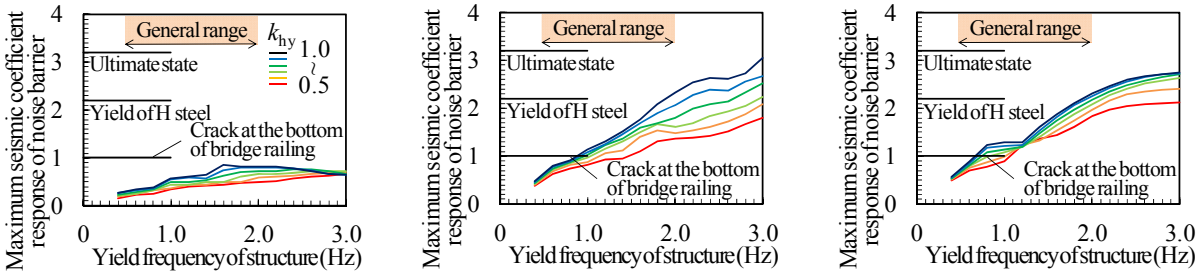

(a) L1(G3) (b) L2speI(G3) (c) L2speII(G3)

Figure 12: Seismic safety of target noise barrier (α_{nbr}=10, f_{nbr}=3.3Hz)

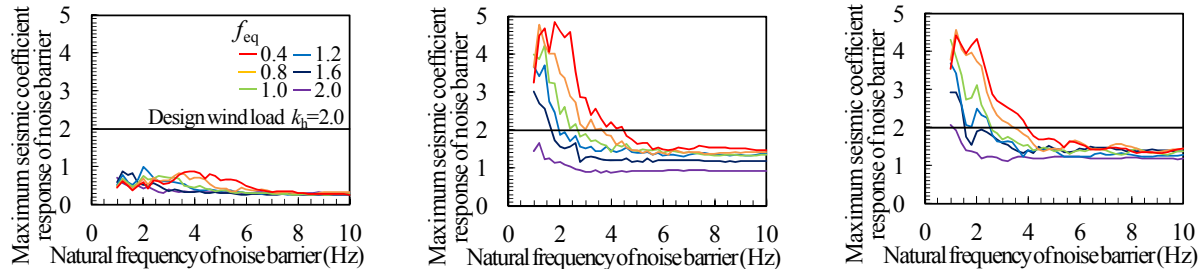

(a) L1(G3) (b) L2speI(G3) (c) L2speII(G3)

Figure 13: Effect of natural frequency of noise barrier f_{nbr} (α_{nbr}=10, k_{hy}=1.0)

Figure 11 shows the maximum seismic coefficient response of the noise barrier which indicates the dynamic interaction between the noise barriers and the structures on the basis of the results of k_{hy}=1.0 and f_{eq}=1.0, 2.0 Hz. As shown in the figure, in the case of f_{eq}=2.0Hz, the seismic coefficient response of the coupled model is larger than that of the divided model in the region of f_{nbr}=1.0~2.0Hz, while the trend has been reversed in the region of f_{nbr}≧2.0Hz. In the case of f_{eq}=1.0Hz, the seismic coefficient response of the coupled model is smaller than that of the divided model in all the region of f_{nbr}≧1.0Hz. In addition, there is a tendency that the response intensity decreases with the decrease of α_{nbr} as a whole. These are because the transfer function of noise barriers varies depending on the interaction between the noise barriers and the structures, and also depend on the magnitude of f_{str} and f_{nbr}.

Therefore, in order to evaluate the seismic response of noise barrier, it is necessary to take account of the influence of the dynamic interaction between the noise barrier and the structure, because the transfer function of the noise barrier substantially depends on the interaction.

3.3. Seismic safety of the noise barrier

Figure 12 shows the maximum seismic coefficient response of the noise barrier which indicates the seismic safety of the noise barrier on the basis of the results of the coupled model of α_{nbr}=10 and f_{nbr}=3.3Hz with C point. As shown in the figure, it can be observed that the maximum response of the noise barriers increases with the increase of f_{eq} or k_{hy}. This is because the resonance between structures and noise barriers occurs when f_{eq} gets closer to f_{nbr} and the input acceleration to the noise barriers increases with the increase of k_{hy}.

Comparing the response value shown in Figure 12 with the limit value shown in Figure 9, in the case of f_{nbr}=3.3Hz and k_{hy}=1.0, L1 earthquake can cause cracks at the location of the cross-section changes because the maximum seismic coefficient response is about 0.8. L2 earthquake can cause to the yield of H-shaped steel which supports the noise barrier because it reaches about 2.3.

Figure 13 shows the maximum seismic coefficient response of noise barrier which indicates the effect of the natural frequency of the noise barrier f_{nbr} on the basis of the results of k_{hy}=1.0 and f_{eq}=0.4~3.0Hz. As shown

in the figure, although the maximum seismic coefficient response is about 0.8 at most during L1 earthquake, it exceeds 2.0 in the region of $f_{nbr} \leqq 5$Hz during L2 earthquake.Therefore, The L2earthquake can provide a severer design condition than the wind load for the noise barriers whose natural frequency is 5Hz or less.

4. CONCLUSIONS

The aim of this study is to understand the dynamic response characteristics of the tall noise barrier during seismicity and to evaluate its seismic safety. Conclusions on the basis of numerical studies are as follows.

1) The noise barrier resonates with the yield frequency of structures during the L2 earthquake, while it resonates with the elastic natural frequency of structures when structures respond elastically in such cases as L1 earthquake. This phenomenon becomes significant with the increase of the seismic yield coefficient.

2) In order to evaluate the seismic response of noise barrier, it is necessary to take account of the influence of the dynamic interaction between the noise barrier and the structure, because the transfer function of the noise barrier substantially depends on the interaction.

3) The fracture morphology of the target noise barrier is such that cracks occurs at the top of bridge railing when seismic coefficient k_{hy} is about 0.4; H-shaped steel exceeds the yield state when it is about 2.2; and the noise barrier reaches the ultimate state when it is about 3.2. The L1 earthquake can cause cracks at the top of bridge railing, and the L2 earthquake can cause the yield of H-section steel which supports the noise barrier.

4) The L2earthquake can provide a severer design condition than the wind load for the noise barriers whose natural frequencies are 5Hz or less.

REFERENCES

Yoshitaka MURONO, Takashi KATO and Akihiro TOYOOKA (2012). Effect of Assessment of viaduct and pole resonance for seismic input level. Journal of Japan Society of Civil Engineers, Ser. A1 (Structural Engineering & Earthquake Engineering). Volume 68. Issue 4. pp. I_418-I_422.

Toshinari IMAMURA, Yoshitaka MURONO, Kimitoshi SAKAI and Tsutomu SATO (2007). Seismic Response Analysis of Coupled System between Railway Viaduct- Power Pole, Journal of Earthquake Engineering, pp.1182-1190.

Hikaru NAKAMURA, Takeshi HIGAI : Compressive Fracture Energy and Fracture Zone Length of Concrete, Modeling of Inelastic Behavior of RC Structures under Seismic Loads, ASCE, pp.471-487, 2001.

Railway Technical Research Institute (2004). Design Standards for Railway Structures and Commentary (Concrete Structures). Maruzen Co., Ltd. Tokyo. (in Japanese).

Railway Technical Research Institute (2012). Design Standards for Railway Structures and Commentary (Seismic Design). Maruzen Co., Ltd. Tokyo. (in Japanese).

Toshikazu TAKEDA, Mete A. Sozen and N. Norby Nielsen (1970). Reinforced Concrete Response to Simulated Earthquakes, Journal of the Structural Division. Vol. 96. No. 12. pp.2557-2573.

Munemasa TOKUNAGA, Masamichi SOGABE, Kiyoshi ASANUMA, Koya MATSUMOTO, Tetsuo SANTO and Yasuhiko TOKUTOMI (2011). Seismic Safety of the Noise barrier on Railway Viaducts. Journal of Railway mechanics, No.15, pp. 156-163.

Munemasa TOKUNAGA, Masamichi SOGABE, Fumiaki UEHAN, Yukihiro TANIMURA, Yoshitaka MURONO and Kiyoshi ONO (2011). An Estimation Method for Equivalent Natural Period with Microtremor Measurement. RTRI REPORT. Vol.25. No.6. pp. 35-40.

Lee YY and Ng CF (1998). Sound insertion loss of stiffened enclosure plates using the finite element method and the classical approach. Journal of Sound and Vibration. 217(2). pp. 239-260.